論文 / 著書情報
Article / Book Information

題目(和文)	四肢動物における生息環境の酸素濃度と指間細胞死の進化的獲得
Title(English)	Environmental oxygen levels and the evolution of interdigital cell death in tetrapods
著者(和文)	CORDEIRO Ingrid R
Author(English)	Ingrid R. Cordeiro
出典(和文)	学位:博士(理学), 学位授与機関:東京工業大学, 報告番号:甲第11243号, 授与年月日:2019年9月20日, 学位の種別:課程博士, 審査員:田中 幹子,本郷 裕一,太田 啓之,木村 宏,川上 厚志
Citation(English)	Degree:Doctor (Science), Conferring organization: Tokyo Institute of Technology, Report number:甲第11243号, Conferred date:2019/9/20, Degree Type:Course doctor, Examiner:,,,,
学位種別(和文)	博士論文
Category(English)	Doctoral Thesis
種別(和文)	要約
Type(English)	Outline

2019 Doctoral Thesis

Thesis Outline

Environmental oxygen levels and the evolution of interdigital cell death in tetrapods

Tokyo Institute of Technology
Graduate School of Bioscience and Biotechnology
Department of Biological Sciences

Ingrid Rosenburg Cordeiro

Advisor: prof. Mikiko Tanaka

TABLE OF CONTENTS

ABSTRACT

Amphibians form fingers without webbings by differential growth between digital and interdigital regions. Amniotes, however, employ interdigital cell death (ICD), an additional mechanism that contributes to a greater variation of limb shapes. Here, I investigate the role of environmental oxygen in the evolution of ICD in tetrapods. While cell death is restricted to the limb margin in amphibians with aquatic tadpoles, *Eleutherodactylus coqui*, a frog with terrestrial direct-developing eggs, has cell death in the interdigital region. Chickens require sufficient oxygen and reactive oxygen species to induce cell death, with the oxygen tension profile itself being distinct between the limbs of chicken and *Xenopus laevis* frogs. Notably, increasing blood vessel density in *X. laevis* limbs, as well as incubating tadpoles under high oxygen levels, induces ICD. I propose that the oxygen available to terrestrial eggs was an ecological feature crucial for the evolution of ICD, made possible by conserved autopod-patterning mechanisms.

1 INTRODUCTION

1.1 Oxygen availability for amphibians and amniotes during development

Tetrapods are all vertebrates with four limbs, which are divided into amphibians (frogs, salamanders and caecilians) and amniotes (reptiles, birds and mammals). A major difference between these groups exist during their development. Some amphibians hatch from their eggs early and live freely as a tadpole or larvae. Then, they undergo metamorphosis and change their body shape to that of an adult individual (**Figure 1A. Biphasic development**). Other amphibians lay eggs on land and an immature adult animal emerges by the end of the embryonic period, without a tadpole stage (**Figure 1B. Direct development**). In both cases, their eggs are covered only by a protective vitelline membrane. In contrast, amniotes have many extraembryonic membranes rich in blood vessels that allow them to exchange gases and nutrients very efficiently. These membranes connect to the egg shell and egg yolk in reptile, birds and egg-laying mammals (**Figure 1C. In the egg**), or with the mother in placental mammals (**Figure 1D. In the uterus**). In addition, egg laying-amniotes have a hard, protective shell that prevents dehydration in the land.

The different developmental strategies of the tetrapods affect how much oxygen is available to these animals. The oxygen available to aquatic animals is the dissolved oxygen gas from the atmosphere. Additionally, as the water is about 50 times more viscous than the air, the exchange of gases with the water requires a greater amount of energy from the animal (Schmidt-Nielsen, 1997). As a result, many aquatic animals form smaller eggs or embryos that require less oxygen and are more tolerant to hypoxia (Seymour, 1999). Amphibian embryos with terrestrial eggs have direct access to the oxygen from the air. Direct developing amphibians have adaptations to obtain more oxygen throughout their development, such as the highly vascularized tails of the coquí frogs (*Eleutherodactylus coqui*; Townsend and Stewart, 1985). In a more extreme adaptation to the terrestrial environment, the amniotes have amniotic membranes. They are rich in blood vessels that provide a large area for gas exchange throughout the whole egg shell – or the placenta, in the case of mammals. This high oxygen availability allows amniotes to have a faster metabolic rate, greater energy requirements and, in birds and mammals, maintain their temperature as warm-blooded animals (Berner et al., 2007; Schmidt-Nielsen, 1997).

1.2 Development of the interdigital regions in amphibians and amniotes

The shape of the autopods – hands and feet – has a critical role in the adaptation of tetrapods to their habitats. Amphibians form fingers without webbing by differential growth patterns between the digits and the areas between them, the interdigital regions (Cameron and Fallon, 1977; Vlaskalin et al., 2004) (**Figure 2A**). However, amniotes require cell death to remove their interdigital webbings during limb development (**Figure 2B**). This additional step contributes to the formation of species-specific features (Cooper et al., 2014; Fallon and Cameron, 1977; Fernández-Terán et al., 2006; Salas-Vidal et al., 2001), including unique morphologies such as the coot leg (*Fulica atra*; Zuzarte-Luis and Hurle, 2005) (**Figure 2B**) and the bat wing (*Carollia perspicillata*; Weatherbee et al., 2006).

Interdigital cell death (ICD) has not been found in previously investigated amphibians (Cameron and Fallon, 1977; Vlaskalin et al., 2004). The only exception is the seepage salamander (*Desmognathus aeneus*), which has apoptotic cells in the interdigital regions (Franssen et al., 2005). However, it is not clear if cell death plays a role in shaping the limbs of this species. Factors responsible for the acquisition of interdigital cell death by tetrapods, and how they were integrated to limb development, are still unknown.

1.3 Molecular control of interdigital cell death (ICD) in amniotes: Bmp signaling and reactive oxygen species (ROS)

Areas of cell death in the limbs of amniotes are regulated by several signaling pathways, which culminate in the activation of Bmp signaling (Gañan et al., 1998; Kaltcheva et al., 2016; Yokouchi et al., 1996; Zou and Niswander, 1996; Zuzarte-Luis and Hurle, 2005). Although the roles of Bmps in patterning the limbs and the skeleton have been studied extensively, the downstream targets of this pathway which are responsible for the induction of cell death are still unknown. Nevertheless, activation of the Bmp pathway somehow leads to the activation of the intrinsic apoptotic pathway as well as permeabilization of the lysosomal membranes (Lorda-Diez et al., 2015).

Other studies have demonstrated that reactive oxygen species (ROS) are also required for cell death in mouse limbs even with an intact genetic background (Salas-Vidal et al., 1998; Schnabel et al., 2006). The amount of blood vessels in the interdigital region was important for the production of ROS and appearance of ICD (Eshkar-Oren et al., 2015). In addition, several recent papers indirectly support an involvement of ROS in this process, revealing the presence of cell senescence in the interdigital region (Storer et al., 2013), phosphorylation of the stress-activated MAP kinases p38 and JNK (Zuzarte-Luíz et al., 2004), expression of stress-regulated AP-1 transcription factors (Suda et al., 2014) and activation of DNA damage pathways (Montero et al., 2016).

Environmental oxygen levels can modulate ROS levels in a tissue-specific way, regulating both developmental processes and adult homeostasis (Covarrubias et al., 2008; Puente et al., 2014; Wagenfuhr et al., 2015). However, the importance of oxygen levels for the evolution of interdigital cell death was not previously investigated. Here, I investigated here how ecological changes may have contributed directly to the evolution of limb shape.

1.4 Bmp signaling during limb development

Bmp proteins belong to the TGFβ superfamily. They bind to the serine/threonine kinase receptors BMPR-I and BMPR-II, which then phosphorylate and activate the SMAD proteins (SMAD1/5/8). The activated SMAD then forms a complex with SMAD4, enters the nucleus and activates the transcription of Bmp target genes, such as *msx2* (**Figure 3A**) (Pignatti et al., 2014). Bmps also mediates a non-canonical pathway in the limbs by activating the stress-activated MAP kinases p38 and the Jun-N Terminal kinase (JNK) (**Figure 3A**) (Gunnel et al., 2010; Zuzarte-Luíz et al., 2004).

Bmp signaling is involved in several steps of the development of the limbs. Bmp signals are expressed in the newly formed autopod, where they are part of a self-regulatory loop that forms a striped pattern of digital and interdigital regions (**Figure 3B; 1. Digit number**). In this system, the areas of the digits express the chondrogenic factor *sox9* and the interdigital region expresses *bmp* and *wnt*, which interact with each other in a Turing pattern (Hiscock et al., 2017; Raspopovic et al., 2014). As Bmps are responsible for the induction of *sox9,* they determine the number of digits (**Figure 3B; 1. Digit number**), loss-of-function experiments during this moment causes the formation of multiple fingers in both amphibians and amniotes (Jones et al., 2013; Norrie et al., 2004; Pignatti et al., 2014).

Bmps remain expressed in the interdigital regions in a next stage, when they regulate the extension of the fingers. This process takes place at the distal tip of the fingers, in a signaling center called the phalanx-forming region (PFR), which regulates the number of bones in each finger (**Figure 3B; 2. Digit identity and cell death**). The number of phalanges in each finger – two in the thumb or toes and three in other fingers, in humans – is called digit identity. Inhibition of Bmp signaling at this stage causes a shortening of the fingers (Suzuki et al., 2008; Montero et al., 2008; Jones et al., 2013; Huang et al., 2016), supporting a role in the extension of the fingers and the formation of the joints. At the same time, Bmps are required for induction of cell death in the interdigital membranes of amniotes, as described in the section 1.4 (**Figure 3B; 2. Digit identity and cell death**); if the Bmp signaling is inhibited in this tissue, the interdigital webbings are maintained (Gañan et al., 1998; Kaltcheva et al., 2016;

Yokouchi et al., 1996; Zou and Niswander, 1996; Zuzarte-Luis and Hurle, 2005). Both ducks (Gañan et al., 1998) and bats (Weatherbee et al., 2003) express the Bmp inhibitor *grem1* in their interdigital regions, leading to the absence of cell death and formation of webbed limbs.

Finally, Bmps remain expressed around the finger cartilages, where they regulate the differentiation of the finger cartilages into bone tissue (**Figure 3B; 3. Skeletogenesis**). Disrupting Bmp signaling at this late stage leads to defects in digit ossification (Chimal-Monroy et al., 2003; Bandyopadhyay et al., 2006).

Taken together, these studies reveal common roles for Bmp signaling in the development of the limb skeleton in both amniotes and amphibians, and a role in inducing interdigital cell death in amniotes.

2 METHODS

2.1 Animals, transgenic frogs and oxygen incubation

All animals were staged according to developmental tables: chicken (*Gallus gallus*; Hamburger and Hamilton, 1951), African clawed frogs (*Xenopus laevis*; Gurdon, 1995), Japanese fire-bellied newts (*Cynops pyrrhogaster*; Okada and Ishikawa, 1947) and coquí frogs (*Eleutherodactylus coqui*; Townsend and Stewart, 1985).

The open reading frame of *X. laevis* VegfA (NM_001097785.1, Genbank) was amplified with primers that included HindIII and Kozak sequences at N-terminus and ClaI and EcoRI sequences at C-terminus and cloned into the ISXexEGFP plasmid (Thermes et al., 2002). The mouse Prrx1 promoter was amplified using primers that included KpnI sequence and HindIII sequences and cloned into the previous plasmid. Transgenic frogs were created by injecting unfertilized eggs with 150 ng of Prrx1-VefgA-EGFP plasmids, sperm nucleus and oocyte extract (Kroll and Amaya, 1996; Ogino et al., 2008).

Incubations under low (5%) or high (65%) oxygen atmosphere were made using a multigas incubator (APM-30D, Astec). Isolated chicken limbs were incubated in Mesenchymal Stem Cell medium (ScienCell Research Laboratories). Tadpoles were incubated either individually in 6-well plates for 3 hr or in 90 mm Petri dishes for 1 wk. N-acetyl-cysteine (Sigma) was dissolved in PBS and used at 1 mg/L.

2.2 Detection of cell death, cell senescence, reactive oxygen species (ROS), blood vessels and RNA expression (in situ hybridization) in whole mount samples

Cell death was detected in non-fixed samples using Lysotracker Red/Green (Thermo Fisher Scientific) (Fogel et al., 2012). Cell senescence was detected in samples fixed in paraformaldehyde 4% overnight at as described before (Debacq-Chainiaux et al., 2009). Reactive oxygen species were detected in non-fixed whole tadpoles or isolated chicken limbs using dihydroethidium (DHE, Sigma-Aldrich) or CellROX Deep Red (Life Technologies). Blood vessels were visualized through intravascular injection of highlighter ink (Takase et al., 2013).

In situ hybridization probes were synthesized as before (Suda et al., 2014). Primers based on sequences of *X. laevis bmp4a* (NM_001088032, Genbank) and *X. laevis msx2* (ENSXETT00000020130, Ensembl) and pGEM-Teasy vectors (Promega) were used. Whole-mount in situ hybridization was performed as described previously (Satoh et al., 2006).

2.3 Immunohistochemistry and measurement of oxygen tension in the tissue

Chicken limbs were fixed overnight with 4% paraformaldehyde/PBS and *X. laevis* limbs were fixed for 3 hr with MEMFA (100 mM MOPS pH 7.4, 2 mM EGTA, 1 mM $MgSO_4$, 3.7% formaldehyde). Samples embedded in OCT were sectioned at 10 µm. Primary antibodies used were anti-8-oxoguanine antibody (1:100, ab 64548, Abcam) and anti-phospho-histone H3 (1:500, 06-570, Millipore), which were detected with anti-mouse IgM/HRP (1:250, sc-2064, Santa Cruz) or goat anti-rabbit Alexa Fluor-594 conjugated antibodies (1:500, 06-570, Millipore). Nuclear counterstaining was performed with Hoechst 33342 solution (H3570, Invitrogen).

Oxygen levels were measured using EF5 compound. 100 µl of 10 mM EF5 solution was pipetted over the chicken embryo, which was then incubated for 3 hr at 37 °C. Alternatively, *X. laevis* tadpoles were kept in Petri dishes with 100 µM EF5 in 0.1% sea-salt solution for 3 hr. Limbs were then fixed for 3 hr with PFA 4% and prepared for immunohistochemistry using ELK3-488 as a described (Koch, 2002).

For further details, please see Cordeiro et al., 2019.

3 RESULTS

3.1 Bmp signaling does not explain differences in ICD between *X. laevis* and amniotes

Firstly, I hypothesized that cell death-promoting Bmp signaling would disappear from the interdigital region of the amphibian *X. laevis* following its role in establishing the digit numbers at stages 52-53 (**Figure 3B; 1. Digit numbers**) (Jones et al., 2013). However, *bmp4* (Satoh et al., 2005) and its target gene *msx2* are expressed in interdigital regions during the subsequent stages 54 and 55 (**Figure 4A**) (Cordeiro et al., 2019). It is possible that this expression is explained by the subsequent role of Bmps in regulating the number of joints in each finger (Jones et al., 2013) (**Figure 3B; 2. Digit identity**). These data suggest that active interdigital Bmp signaling is not sufficient to determine if ICD is present in tetrapod limbs, and an additional factor is required.

3.2 The distribution of cell death, reactive oxygen species (ROS), cell senescence and oxidative damage is correlated in tetrapod limbs

As ROS are required for ICD in mice (Eshkar-Oren et al., 2015; Salas-Vidal et al., 1998; Schnabel et al., 2006), their pattern in other tetrapods was investigated. Chickens have extensive cell death and ROS production in the interdigital region. In contrast, *X. laevis* frogs have dying cells and high ROS production only in the border of their limbs (Cordeiro et al., 2019). The same pattern is observed for cells containing the oxidized form of guanine that indicates presence of oxidative damage, 8-oxoguanine. In addition, senescent cells, a form of proliferative arrest induced by several stresses including exposure to oxidants (Childs et al., 2014), were distributed throughout the chicken interdigital region, but only limb margins of *X. laevis*. Taken together, these data indicate that markers of oxidative stress are correlated with areas of cell death in the limbs of both an amniote and an amphibian (**Figure 4B**) (Cordeiro et al., 2019).

3.3 Oxygen and ROS regulate ICD in chicken and *X. laevis*

To understand if ROS can regulate cell death in an amniote, chicken forelimbs were incubated in culture medium with PBS (left limbs, as a control) or the ROS inhibitor N-acetyl-cysteine (NAC, right limbs). The ROS inhibitor decreased the number of dying cells in the wings in comparison with the control, indicating that ROS are not only a byproduct of cell death in the limb. Next, a possible role of atmospheric oxygen in modulating ICD was tested using a multi-gas incubator. Incubating chicken limbs under hypoxia (5% oxygen) is sufficient to inhibit cell death in the interdigital mesenchyme in comparison with control limbs (21% oxygen). Conversely, incubation under hyperoxia (60% oxygen) increases the number of Lysotracker-positive cells specifically in the interdigital region. Thus, oxygen levels regulate ICD in chicken limbs (**Figure 5A**) (Cordeiro et al., 2019).

Given its inductive role in chicken limbs, I tested if increased environmental oxygen could promote cell death in the interdigital region of an amphibian, *X. laevis*. As a reference, the atmospheric air contains 21% of oxygen (or 209.460 parts per million or ppm) and the aquariums where the tadpoles are kept have 8.6 ± 0.45 ppm (S.D., n = 5) of dissolved oxygen, because the water is kept oxygenated by an air pump. Tadpoles were incubated in shallow Petri dishes in which the water depth was 1.8 cm; a constant depth is important to avoid variation in the levels of dissolved oxygen, which is higher closer to the surface. Under these conditions, hyperoxia provided an approximately threefold increase in the amount of dissolved oxygen in the water around the tadpoles (from 7.9 ± 0.7 ppm, S.D., n = 5; to 22.2 ± 1.3 ppm, S.D., n = 5).

After 3 hours, a patch of cell death appeared specifically across the interdigital region under hyperoxia, but not normoxia (**Figure 5B**) (Cordeiro et al., 2019). Cell death is accompanied by increased ROS

production. Interestingly, the ectopic ICD can be detected at late stage 54 and stage 55 tadpoles, but not at other stages. These correspond to the stages when Bmp signaling is still active, highlighting a possible common mechanism for ICD across tetrapods.

The effect of hyperoxia was specific to the hindlimbs: there were no ectopic regions of cell death in the tadpole body, while already described regions of cell death, such as the olfactory organs (Dittrich et al., 2016), are present in both conditions. Besides, no ectopic cell death is found in the forelimbs, which form no membranes in the *X. laevis* frogs. The cell proliferation rates are not changed by the higher oxygen levels, neither is the expression of the Bmp target gene *msx2*. Incubating the tadpoles under high oxygen for one week induces a mild reduction of the interdigital membranes in some limbs, defined as limb sinuosity (Jaekel and Wake, 2007), although no statistical significance is found (Cordeiro et al., 2019). Thus, environmental oxygen levels directly affect ROS production within the limb, even promoting ICD in an amphibian that typically lacks it. However, a direct role of cell death in shaping amphibian limbs is not expected, as will be discussed later.

3.4 Blood vessel remodeling is correlated with stages permissive to cell death in tetrapods

Besides atmospheric oxygen levels, blood vessels are also essential for tissue oxygenation. Blood vessel remodeling is the maturation of the existing vessels into a more efficient network, what improves oxygen delivery (Potente et al., 2011) and is correlated with the onset of ICD in mice (Eshkar-Oren et al., 2015). I considered whether the timing of blood remodeling was distinct between chicken and *X. laevis*.

For this, the vasculature of these two species was observed across several stages of limb development. Remodeling is first evident around the finger condensations in both chicken and *X. laevis*. A hierarchically branched network forms in the interdigital region of chicken during ICD stages. Importantly, vascular remodeling also occurs in the *X. laevis* interdigital region during the stages when ICD can be induced by high oxygen levels (Cordeiro et al., 2019). Remodeling progressed in a similar manner throughout limb development in both chicken and *X. laevis* and also coincided with active Bmp signaling. These data highlight how a common potential mechanism for the induction of ICD under sufficient oxygen levels may be shared among tetrapods.

3.5 Increasing limb vasculature density promotes ICD in *X. laevis*

To test directly if blood vessel density can induce ICD in an amphibian, transgenic *X. laevis* with an increased number of blood vessels in the limbs were created. These frogs overexpressed the angiogenic factor *VegfA-b* under the control of the mouse limb-specific promoter *Prrx1* (Martin and Olson, 2000; Suzuki et al., 2007). Reporter expression is observed throughout the limb bud mesenchyme. When compared to wild-type tadpoles, *Prrx1-VegfA-EGFP* tadpoles have increased blood vessel density in the limbs at early stage 54. Increased ROS production is also observed at the same stage. No difference in cell proliferation is observed between wild-type and transgenic hind limbs. Transgene expression decreases as tissues differentiate (Suzuki et al., 2007), and by stage 56 the vasculature is not significantly different from that in wild-type limbs (Cordeiro et al., 2019).

Notably, at late stage 54, all *Prrx1-VegfA-EGFP* tadpoles have ectopic patches of cell death specifically in the interdigital mesenchyme (**Figure 5C**) (Cordeiro et al., 2019). The ectopic cell death is detected in interdigital spaces 1 and 2, consistent with the stronger anterior expression of the transgene at this stage. Cells with high ROS production are also observed in the same region. Thus, increasing the density of blood vessels – the source of oxygen in the limbs – promotes cell death specifically in the interdigital mesenchyme of *X. laevis*.

3.6 The correlation between ICD and environmental oxygen levels is conserved in other amphibians

To add a comparative perspective, the distribution of cell death and ROS was assessed in two other amphibian species: the Japanese fire-bellied newt, *Cynops pyrrhogaster*, and the coquí frog, *Eleutherodactylus coqui*. In *C. pyrrhogaster*, sparse Lysotracker-positive cells are found around the growing digits, as detected in another newt (Vlaskalin et al., 2004). Dying cells were not found in the interdigital region at stage 53, when the fingers had just started to grow, or later at stage 57 (**Figure 6**) (Cordeiro et al., 2019). ROS production was also restricted to those cells. Blood vessels in *C. pyrrhogaster* autopods were found only around the growing digits and did not extend into the interdigital region.

In contrast, cell death is detected in the interdigital regions and limb margins of *E. coqui*. Both Lysotracker-positive and surrounding cells in the interdigital mesenchyme have increased ROS production (**Figure 6**) (Cordeiro et al., 2019), as seen in chicken. Blood vessels of *E. coqui* extend over a large area of the interdigital region. I detected a small number of Lysotracker-positive cells at all times due to their large cell size in relation to overall limb size, a pattern similar to that reported in the seepage salamander, *Desmognathus aeneus*, the only other amphibian species in which ICD has been observed (Franssen et al., 2005).

There is an important ecological difference between these species at the stages when limbs are developing. Both *E. coqui* and *D. aeneus* have direct development (**Figure 1B**): fertilized eggs are laid on land, and an immature adult animal emerges at the end of the embryonic period (Hanken et al., 2001). This life history is more comparable to that seen in amniotes than it is to the biphasic life history (**Figure 1B**), which includes aquatic tadpoles and is characteristic of *X. laevis*, *C. pyrrhogaster* (here) and all other amphibian species in which cell death has been investigated, including *Ambystoma maculatum*, *A. mexicanum, Bufo americanus*, *Notophthalmus viridescens* and *Taricha torosa* (Cameron and Fallon, 1977; Vlaskalin et al., 2004). Thus, high oxygen availability is correlated with the presence of cell death during limb development of tetrapods (**Figure 6**).

3.7 The oxygen profile of the limbs is distinct between chicken and *X. laevis* and can be modulated experimentally

In light of the above results, it would be important to understand how the different oxygen levels surrounding the embryo or tadpole translated to a tissue level during limb development. For this, I measured the oxygen tension profiles of the tissues by using EF5, which binds to proteins only under hypoxia and is then recognized by ELK3 antibodies (Koch, 2002). ELK3 antibodies previously saturated with its ligand EF5 were used as a control, the “competed” stain (Koch, 2002).

Chicken limbs have a high oxygen tension in the interdigital region (**Figure 4C**) (Cordeiro et al., 2019), with levels that reach the upper limit that this method can detect: at least 1% oxygen concentration in the tissue, when no EF5 binding is found (Koch, 2002). In contrast, lower oxygen levels were found in the digits and, as described in mice (Provot et al., 2007), in the joints. Additionally, hypoxia was observed in the distal mesenchyme, which promote the growth the limbs at early stages, and in phalanx-forming regions, which promote growth of the fingers at a later moment (Cordeiro et al., 2019).

Next, I investigated oxygen distribution in the limbs of *X. laevis*. It is not possible to directly compare fluorescence levels among species due to possible differences in the uptake of EF5, but it is possible to compare the staining pattern. In a striking difference from chicken, the interdigital regions of *X. laevis* are hypoxic, even if mild hypoxia is also observed in the fingers (**Figure 4C**) (Cordeiro et al., 2019). Low oxygen tension is detected in the interdigital region as soon as the digit-interdigit pattern becomes evident at stage 52 and continues in subsequent stages. Other landmarks of digit development, however, have an oxygen profile similar to that observed in chicken: the distal

mesenchyme of the limb buds, the phalanx-forming regions and the joints are also hypoxic in *X. laevis*. (Cordeiro et al., 2019) These data reveal that the oxygen tension profile of the interdigital region, but not of other limb structures, is distinct between chicken and *X. laevis*.

Finally, it was evaluated experimentally if the oxygen concentration in the tissue is responsive to environmental oxygen levels. Incubation of limbs under hypoxia, which inhibits cell death in chicken limbs, reduces tissue oxygen tension specifically in their interdigital mesenchyme (Cordeiro et al., 2019). On the other hand, incubating *X. laevis* tadpoles under hyperoxia – a condition that induces ectopic ICD – increases oxygen tension in the interdigital region (Cordeiro et al., 2019). Thus, oxygen tension of the interdigital region, a highly vascularized tissue, is correlated with environmental oxygen levels that surround the embryo or tadpole.

4 DISCUSSION

4.1 Features of digit patterning make the interdigital region permissive to cell death

Here, I propose that the life history strategy regulates oxygen levels in the limbs, with high oxygen levels being necessary for the appearance of cell death in the interdigital region.

One key aspect of this hypothesis is understanding why the amphibian interdigital region is permissive for the induction of cell death, even in species in which cell death does not normally occur. Bmp signaling and a blood vessel remodeling are independently related to ICD in amniotes, as suggested by results of transgenic mouse studies (Eshkar-Oren et al., 2015; Kaltcheva et al., 2016) and those reported here (Cordeiro et al., 2019).

Bmps are expressed in the interdigital regions of both amniotes (Fernandes-Téran et al., 2006. Gañan et al., 1998; Kaltcheva et al., 2016; Yokouchi et al., 1996; Zou and Niswander, 1996) and amphibians (Gross et al., 2011; Guimond et al., 2010; Satoh et al., 2006). Bmp signaling in the interdigital region is part of a self-regulatory network that patterns both digit number and identity in tetrapods (**Figure 3B**) (Hiscock et al., 2017; Huang et al., 2016; Jones et al., 2013; Montero et al., 2008; Onimaru et al., 2016; Raspopovic et al., 2014; Suzuki et al., 2008). Inhibition of Bmps also causes generalized defects in chondrogenesis in both amniotes and amphibians (**Figure 3B**) (Chimal-Monroy et al., 2003; Bandyopadhyay et al., 2006; Jones et al., 2013), suggesting that finger patterning was at least part of the ancestral role of Bmps in the hands and feet prior to the appearance of ICD (**Figure 7A**).

Likewise, vascular patterning is a fundamental feature of skeletal morphogenesis, which is induced by signals from the emerging cartilages (Eshkar-Oren et al., 2009), which form a vascular plexus required for ossification during later stages (Ferrara et al., 1999; Zelzer et al., 2002). In the hands and feet, remodeling signals from the digit cartilages extend to the interdigital region and creates areas of high local oxygen availability (Eshkar-Oren et al., 2015) (**Figure 7B**).

It is fascinating to speculate that an independent developmental step, ICD, might have emerged from two preexisting traits of digit morphogenesis in the presence of increased environmental oxygen levels (Cordeiro et al., 2019).

4.2 Terrestrial eggs increased oxygen availability during evolution

While all animals are adapted to obtain oxygen from their respective environments, the air's increased oxygen content and decreased mass in comparison to water makes air-breathing more efficient (Schmidt-Nielsen, 1997); hyperoxia alone has a positive effect on vertebrate developmental rate and body size (Berner et al., 2007). However, increased environmental oxygen also has deleterious effects, such as loss of the heart regenerative potential in the mammalian heart as a consequence of the oxygen-rich postnatal environment (Puente et al., 2014). Balancing the positive and negative effects of ROS appears to have been a critical step in the invasion of oxygenated settings by animals as a whole, as ROS are regulators of cell proliferation, differentiation and death (Covarrubias et al., 2008; Hammarlund et al., 2018). Consistent with this idea, lower oxygen levels were observed in the apical ectodermal ridge (AER) and phalanx-forming region (Cordeiro et al., 2019), two highly proliferating tissues that regulate the extension of the limbs and fingers, respectively (Montero et al., 2008; Summerbell et al., 1973; Suzuki et al., 2008).

I propose that terrestrial direct development is causally associated with increased oxygen availability and ICD in tetrapods, but it remains to be determined if cell death was initially only a byproduct of increased ROS levels or a preexisting adaptive feature (**Figure 6**). For instance, tropical salamanders (*Bolitoglossa* spp.) evolved webbed feet multiple times, mostly as a consequence of the evolution of correlated traits and not as the primary targets of adaptation (Jaekel and Wake, 2007). The very mild

reduction of the interdigital webbing in *X. laevis* incubated for one week under hyperoxia (**Figure 8E**) indicates that ICD may not yet be integrated to other limb patterning mechanisms in amphibians (**Figure 6**). In the same way, whether cell death plays a role in limb morphogenesis of *E. coqui* (Cordeiro et al., 2019) or *D. aeneus* (Franssen et al., 2005) is presently unknown. Hence, investigating additional direct-developing species (Wake and Hanken, 1996), as well as determining why the differential tissue growth employed by amphibians was insufficient to remove the interdigital region in amniotes (Cameron and Fallon, 1977; Salas-Vidal et al., 2001), will be essential to fully elucidate the origins of cell death as a novel step in the evolution of limb development in amniotes.

REFERENCES

Bandyopadhyay, A., Tsuji, K., Cox, K., Harfe, B.D., Rosen, V., and Tabin, C.J. (2006). Genetic analysis of the roles of BMP2, BMP4, and BMP7 in limb patterning and skeletogenesis. PLoS Genet. *2*, 2116–2130.

Berner, R., VandenBrooks, J., and Ward, P. (2007). Oxygen and evolution. Science *316*, 557–559.

Cameron, J.A., and Fallon, J.F. (1977). The absence of cell death during development of free digits in amphibians. Dev. Biol. *55*, 331–338.

Childs, B.G., Baker, D.J., Kirkland, J.L., Campisi, J. and van Deursen, J.M. (2014). Senescence and apoptosis: dueling or complementary cell fates? EMBO Reports *15*, 1139–1153.

Chimal-Monroy, J., Rodriguez-Leon, J., Montero, J.A., Gañan, Y., Macias, D., Merino, R., and Hurle, J.M. (2003). Analysis of the molecular cascade responsible for mesodermal limb chondrogenesis: Sox genes and BMP signaling. Dev. Biol. *257*, 292–301.

Cooper, K.L., Sears, K.E., Uygur, A., Maier, J., Baczkowski, K.-S., Brosnahan, M., Antczak, D., Skidmore, J.A., and Tabin, C.J. (2014). Patterning and post-patterning modes of evolutionary digit loss in mammals. Nature *511*, 41–45.

Cordeiro, I.R., Kabashima, K., Ochi, H., Munakata, K., Nishimori, C., Laslo, M., Hanken, J. and Tanaka, M. Environmental oxygen exposure allows for the evolution of interdigital cell death in limb patterning (2019). Dev. Cell *50*, 155–166.

Covarrubias, L., Hernández-García, D., Schnabel, D., Salas-Vidal, E., and Castro-Obregón, S. (2008). Function of reactive oxygen species during animal development: Passive or active? Dev. Biol. *320*, 1–11.

Debacq-Chainiaux F., Erusalimsky, J.D., Campisi, J. and Toussaint, O. (2009) Protocols to detect senescence associated beta-galactosidase (SA- βgal) activity, a biomarker of senescent cell in culture and in vivo. Nat Protoc *4*, 1798–1806.

Dittrich, K., Kuttler, J., Hassenklöver, T., and Manzini, I. (2016). Metamorphic remodeling of the olfactory organ of the African clawed frog, *Xenopus laevis*. J. Comp. Neurol. *524*, 986–998.

Eshkar-Oren, I., Viukov, S. V., Salameh, S., Krief, S., Oh, C.-d., Akiyama, H., Gerber, H.-P., Ferrara, N., and Zelzer, E. (2009). The forming limb skeleton serves as a signaling center for limb vasculature patterning via regulation of Vegf. Development *136*, 1263–1272.

Eshkar-Oren, I., Krief, S., Ferrara, N., Elliott, A.M., and Zelzer, E. (2015). Vascular patterning regulates interdigital cell death by a ROS-mediated mechanism. Development *142*, 672–680.

Fallon, J.F., and Cameron, J. (1977). Interdigital cell death during limb development of the turtle and lizard with an interpretation of evolutionary significance. J. Embryol. Exp. Morphol. *40*, 285–289.

Fernández-Terán, M.A., Hinchliffe, J.R., and Ros, M.A. (2006). Birth and death of cells in limb development: A mapping study. Dev. Dyn. *235*, 2521–2537.

Ferrara, N., Gerber, H.-P., Vu, T.H., Ryan, A.M., Kowalski, J., and Werb, Z. (1999). VEGF couples hypertrophic cartilage remodeling, ossification and angiogenesisduring endochondral bone formation. Nat. Med. *5*, 623–628.

Fogel, J.L., Thein, T.Z.T., and Mariani, F. V (2012). Use of LysoTracker to detect programmed cell death in embryos and differentiating embryonic stem cells. J. Vis. Exp. *68*, 4254.

Franssen, R.A., Marks, S., Wake, D., and Shubin, N. (2005). Limb chondrogenesis of the seepage salamander, *Desmognathus aeneus* (Amphibia: Plethodontidae). J. Morphol. *265*, 87–101.

Gañan, Y., Macias, D., Basco, R.D., Merino, R., and Hurle J.M. (1998) Morphological diversity of the avian foot is related with the pattern of msx gene expression in the developing autopod. Dev Biol. *196*, 33–41.

Gross, J.B., Kerney, R., Hanken, J., and Tabin, C.J. (2011). Molecular anatomy of the developing limb in the coquí frog, *Eleutherodactylus coqui*. Evol. Dev. *13*, 415–426.

Guimond, J.-C., Lévesque, M., Michaud, P.-L., Berdugo, J., Finnson, K., Philip, A., and Roy, S. (2010). BMP-2 functions independently of SHH signaling and triggers cell condensation and apoptosis in regenerating axolotl limbs. BMC Dev. Biol. *10*, 15.

Gunnell, L.M., Jonason, J.H., Loiselle, A.E., Kohn, A., Schwarz, E.M., Hilton, M.J. and O'Keefe, R.J. (2010). TAK1 Regulates Cartilage and Joint Development via the MAPK and BMP Signaling Pathways J. Bone Miner. Res. *25*, 1784–1797.

Gurdon, J.B. (1995). Normal table of *Xenopus laevis* (Daudin). Trends Genet. *11*, 418.

Hamburger, V., and Hamilton, H.L. (1951). A series of normal stages in the development of the chick embryo. J. Morphol. *88*, 49–92.

Hammarlund, E.U., von Stedingk, K., and Påhlman, S. (2018). Refined control of cell stemness allowed animal evolution in the oxic realm. Nat. Ecol. Evol. *2*, 220–228.

Hanken, J., Carl, T.F., Richardson, M.K., Olsson, L., Schlosser, G., Osabutey, C.K., and Klymkowsky, M.W. (2001). Limb development in a “nonmodel” vertebrate, the direct-developing frog *Eleutherodactylus coqui*. J. Exp. Zool. (Mol. Dev. Evol.) *291*, 375–388.

Hiscock, T.W., Tschopp, P., and Tabin, C.J. (2017). On the formation of digits and joints during limb development. Dev. Cell *41*, 459–465.

Huang, B.L., Trofka, A., Furusawa, A., Norrie, J.L., Rabinowitz, A.H., Vokes, S.A., Mark Taketo, M., Zakany, J., Mackem, S., Taketo, M.M., et al. (2016). An interdigit signalling centre instructs coordinate phalanx-joint formation governed by 5’Hoxd-Gli3 antagonism. Nat. Commun. *7*, 1–10.

Jaekel, M., and Wake, D.B. (2007). Developmental processes underlying the evolution of a derived foot morphology in salamanders. Proc. Natl. Acad. Sci. U.S.A. *104*, 20437.

Jones, T.E.M., Day, R.C., and Beck, C.W. (2013). Attenuation of bone morphogenetic protein signaling during amphibian limb development results in the generation of stage-specific defects. J. Anat. *223*, 474–488.

Kaltcheva, M.M., Anderson, M.J., Harfe, B.D., and Lewandoski, M. (2016). BMPs are direct triggers of interdigital programmed cell death. Dev. Biol. *411*, 266–276.

Koch, C.J. (2002). Measurement of absolute oxygen levels in cells and tissues using oxygen sensors and 2-nitroimidazole EF5. Methods Enzymol. *352*, 3–31.

Kroll, K.L., and Amaya, E. (1996). Transgenic *Xenopus* embryos from sperm nuclear transplantations reveal FGF signaling requirements during gastrulation. Development *122*, 3173–3183.

Longair, M.H., Baker, D.A., and Armstrong, J.D. (2011). Simple Neurite Tracer: Open Source software for reconstruction, visualization and analysis of neuronal processes. Bioinformatics *27*, 2453–2454.

Lorda-Diez, C.I., Montero, J.A., Garcia-Porrero, J.A., and Hurle, J.M. (2015). Interdigital tissue regression in the developing limb of vertebrates. Int. J. Dev. Biol. *59*, 55–62.

Martin, J.F., and Olson, E.N. (2000). Identification of a *prx1* limb enhancer. Genesis *26*, 225–229.

Montero, J.A., Sanchez-Fernandez, C., Lorda-Diez, C.I., Garcia-Porrero, J.A., and Hurle, J.M. (2016). DNA damage precedes apoptosis during the regression of the interdigital tissue in vertebrate embryos. Sci Rep. *6*, 35478.

Montero, J.A., Lorda-Diez, C.I., Gañan, Y., Macias, D., and Hurle, J.M. (2008). Activin/TGFβ and BMP crosstalk determines digit chondrogenesis. Dev. Biol. *321*, 343–356.

Norrie, J.L., Lewandowski, J.P., Bouldin, C.M., Amarnath, S., Li, Q., Vokes, M.S., Ehrlich, L.I.R., Harfe, B.D., and Vokes, S.A. (2014). Dynamics of BMP signaling in limb bud mesenchyme and polydactyly. Dev. Biol. *393*, 270–281.

Ogino, H., Fisher, M., and Grainger, R.M. (2008). Convergence of a head-field selector Otx2 and Notch signaling: a mechanism for lens specification. Development *135*, 249–258.

Okada, Y.K., and Ishikawa, M. (1947). Normal table of Triturus pyrrphogaster. Jpn. J. Exp. Morphol. *3*, 1–6.

Onimaru, K., Marcon, L., Musy, M., Tanaka, M., and Sharpe, J. (2016). The fin-to-limb transition as the re-organization of a Turing pattern. Nat. Commun. *7*, 1–9.

Pignatti, E., Zeller, R., and Zuniga, A. (2014). To BMP or not to BMP during vertebrate limb bud development. Semin. Cell Dev. Biol. *32*, 119–127.

Potente, M., Gerhardt, H., and Carmeliet, P. (2011). Basic and therapeutic aspects of angiogenesis. Cell *146*, 873–887.

Provot, S., Zinyk, D., Gunes, Y., Kathri, R., Le, Q., Kronenberg, H.M., Johnson, R.S., Longaker, M.T., Giaccia, A.J., and Schipani, E. (2007). Hif-1α regulates differentiation of limb bud mesenchyme and joint development. J. Cell Biol. *177*, 451–464.

Puente, B.N., Kimura, W., Muralidhar, S.A., Moon, J., Amatruda, J.F., Phelps, K.L., Grinsfelder, D., Rothermel, B.A., Chen, R., Garcia, J.A., et al. (2014). The oxygen-rich postnatal environment induces cardiomyocyte cell-cycle arrest through DNA damage response. Cell *157*, 565–579.

Raspopovic, J., Marcon, L., Russo, L., and Sharpe, J. (2014). Digit patterning is controlled by a Bmp-Sox9-Wnt Turing network modulated by morphogen gradients. Science *345*, 566–570.

Salas-Vidal, E., Lomelí, H., Castro-Obregón, S., Cuervo, R., Escalante-Alcalde, D., and Covarrubias, L. (1998). Reactive oxygen species participate in the control of mouse embryonic cell death. Exp. Cell Res. *238*, 136–147.

Salas-Vidal, E., Valencia, C., and Covarrubias, L. (2001). Differential tissue growth and patterns of cell death in mouse limb autopod morphogenesis. Dev. Dyn. *220*, 295–306.

Satoh, A., Suzuki, M., Amano, T., Tamura, K., and Ide, H. (2005). Joint development in *Xenopus laevis* and induction of segmentations in regenerating froglet limb (spike). Dev. Dyn. *233*, 1444–1453.

Satoh, A., Endo, T., Abe, M., Yakushiji, N., Ohgo, S., Tamura, K., and Ide, H. (2006). Characterization of *Xenopus* digits and regenerated limbs of the froglet. Dev. Dyn. *235*, 3316–3326.

Schmidt-Nielsen, K. (1997). Part one: Oxygen. In Animal Physiology: Adaptation and Environment, (Cambridge University Press), pp. 5–122.

Schnabel, D., Salas-Vidal, E., Narváez, V., Sánchez-Carbente, M. del R., Hernández-García, D., Cuervo, R., and Covarrubias, L. (2006). Expression and regulation of antioxidant enzymes in the developing limb support a function of ROS in interdigital cell death. Dev. Biol. *291*, 291–299.

Seymour, R.S. (1999). Respiration of Aquatic and Terrestrial Amphibian Embryos. Amer. Zool. *39*, 261–270.

Storer, M., Mas, A., Robert-Moreno, A., Pecoraro, M., Ortells, M.C., Di Giacomo, V., Yosef, R., Pilpel, N., Krizhanovsky, V., Sharpe, J., and Keyes, W.M. (2013). Senescence is a developmental mechanism that contributes to embryonic growth and patterning. Cell *155*, 1119–1130.

Suda, N., Itoh, T., Nakato, R., Shirakawa, D., Bando, M., Katou, Y., Kataoka, K., Shirahige, K., Tickle, C., and Tanaka, M. (2014). Dimeric combinations of MafB, cFos and cJun control the apoptosis-survival balance in limb morphogenesis. Development *141*, 2885–2894.

Summerbell, D., Lewis, J.H., and Wolpert, L. (1973). Positional information in chick limb morphogenesis. Nature *244*, 492–496.

Suzuki, M., Satoh, A., Ide, H., and Tamura, K. (2007). Transgenic *Xenopus* with prx1 limb enhancer reveals crucial contribution of MEK/ERK and PI3K/AKT pathways in blastema formation during limb regeneration. Dev. Biol. *304*, 675–686.

Suzuki, T., Hasso, S.M., and Fallon, J.F. (2008). Unique SMAD1/5/8 activity at the phalanx-forming region determines digit identity. Proc. Natl. Acad. Sci. U.S.A. *105*, 4185–4190.

Takase, Y., Tadokoro, R., and Takahashi, Y. (2013). Low cost labeling with highlighter ink efficiently visualizes developing blood vessels in avian and mouse embryos. Dev. Growth Differ. *55*, 792–801.

Thermes, V., Grabher, C., Ristoratore, F., Bourrat, F., Choulika, A., Wittbrodt, J., and Joly, J.S. (2002). I-SceI meganuclease mediates highly efficient transgenesis in fish. Mech. Dev. *118*, 91–98.

Townsend, D.S., and Stewart, M.M. (1985). Direct development in *Eleutherodactylus coqui* (Anura: Leptodactylidae): A staging table. Copeia *1985*, 423.Vlaskalin, T., Wong, C.J., and Tsilfidis, C. (2004). Growth and apoptosis during larval forelimb development and adult forelimb regeneration in the newt (*Notophthalmus viridescens*). Dev. Genes Evol. *214*, 423–431.

Vlaskalin, T., Wong, C.J., and Tsilfidis, C. (2004). Growth and apoptosis during larval forelimb development and adult forelimb regeneration in the newt (*Notophthalmus viridescens*). Dev. Genes Evol. *214*, 423–431.

Wagenfuhr, L., Meyer, A.K., Braunschweig, L., Marrone, L., and Storch, A. (2015). Brain oxygen tension controls the expansion of outer subventricular zone-like basal progenitors in the developing mouse brain. Development *142*, 2904–2915.

Wake, D.B., and Hanken, J. (1996). Direct development in the lungless salamanders: What are the consequences for developmental biology, evolution and phylogenesis? Int. J. Dev. Biol. *40*, 859–869.

Weatherbee, S.D., Behringer, R.R., Rasweiler, J.J. 4th, and Niswander, L.A. (2006). Interdigital webbing retention in bat wings illustrates genetic changes underlying amniote limb diversification. Proc. Natl. Acad. Sci. USA. *103*, 15103–15107.

Yokouchi, Y., Sakiyama, J., Kameda, T., Iba, H., Suzuki, A., Ueno, N., and Kuroiwa, a (1996). BMP-2/-4 mediate programmed cell death in chicken limb buds. Development *122*, 3725–3734.

Zelzer, E., McLean, W., Ng, Y.-S., Fukai, N., Reginato, A.M., Lovejoy, S., D'Amore, P.A., and Olsen, B.R. (2002). Skeletal defects in VEGF(120/120) mice reveal multiple roles for VEGF in skeletogenesis. Development *129*, 1893–1904.

Zou, H., and Niswander, L. (1996). Requirement for BMP signaling in interdigital apoptosis and scale formation. Science *272*, 738–741.

Zuzarte-Luís, V., Montero, J.A., Rodriguez-León, J., Merino, R., Rodríguez-Rey, J.C., and Hurlé, J.M. (2004). A new role for BMP5 during limb development acting through the synergic activation of Smad and MAPK pathways. Dev. Biol. *272*, 39–52.

Zuzarte-Luis, V., and Hurle, J.M. (2005). Programmed cell death in the embryonic vertebrate limb. Semin. Cell Dev. Biol. *16*, 261–269.

LIST OF ATTACHED FIGURES

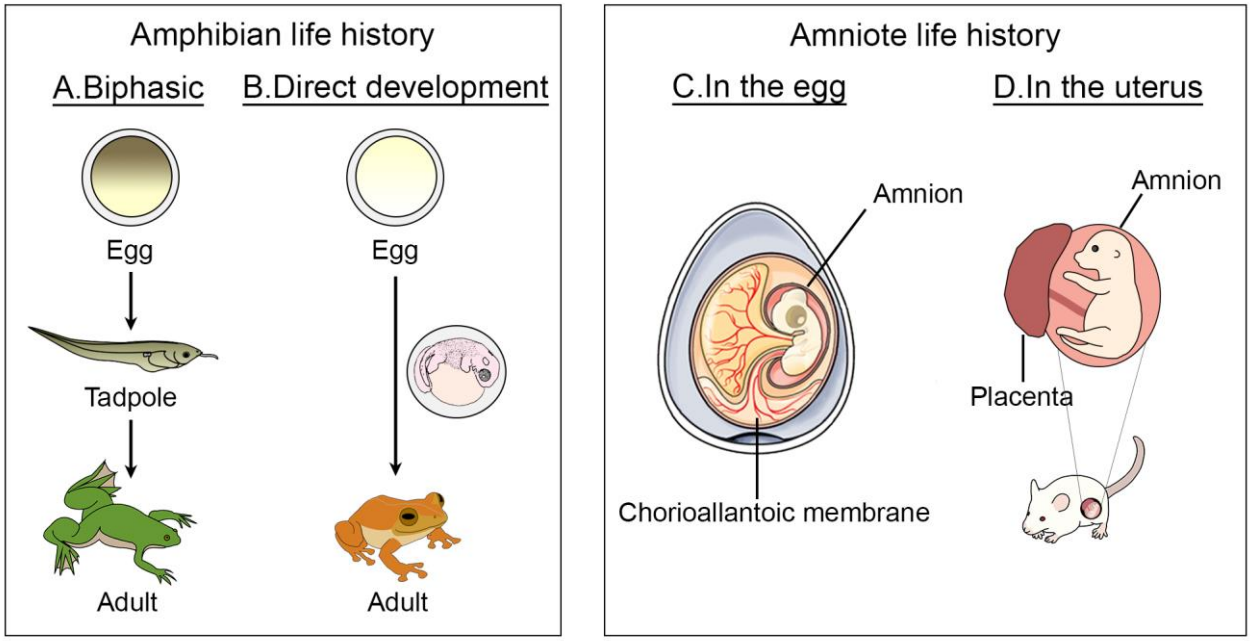

Figure 1. Limb morphology and development of the tetrapods.

Amphibians have two different life history strategies. (**A**) In a biphasic life history, the amphibian eggs hatch early during development into a free-living tadpole. Most tadpoles are aquatic. Later, they undergo metamorphosis into the adult form. (**B**) Amphibians with direct development have no defined metamorphosis. They develop more slowly in the egg, and hatch as an individual with adult shape.

Amniotes have a life history similar to amphibians with direct development. A major difference is the presence of membranes specialized in exchanging oxygen, an adaptation for terrestrial life. (**C**) Reptiles, birds and egg-laying mammals obtain oxygen through the chorioallantoic membranes, which are in contact with the egg shell. (**D**) Mammals in the uterus obtain oxygen from the mother instead, via the placenta, an equivalent to the chorioallantoic membrane.

The chicken egg cartoon is from Wikicommons.

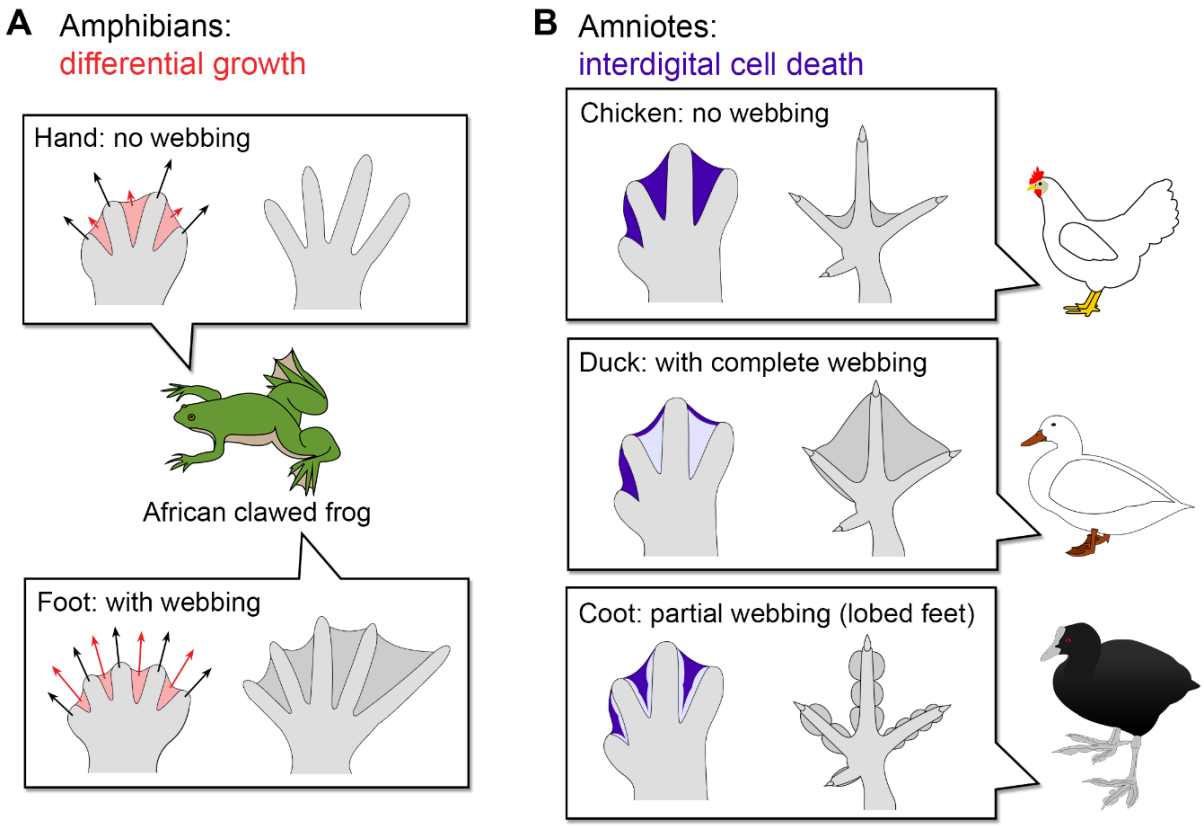

Figure 2. Development of the interdigital regions in amphibians and amniotes.

Cartoons illustrating strategies to shape the interdigital regions during development. Images to the left represent the limbs during development and images to the right indicate the adult shape.

(**A**) The balance between growth of the digits (black arrows) and interdigital regions (red arrows) determine if the hands and feet will form a webbing in amphibians. In the African clawed frog, the hands have no webbings, with little cell proliferation in the interdigital regions (in red). In contrast, the feet have webbings that grow during limb development and are maintained in the adult.

(**B**) Amniotes employ another strategy: their interdigital regions are actively removed by cell death (dark blue), forming fingers free of webbings as observed in chicken feet. In some species, inhibition of cell death (light blue) was important for the evolution of new limb shapes: duck feet have a complete membrane between their fingers, while coot feet have only a partial membrane.

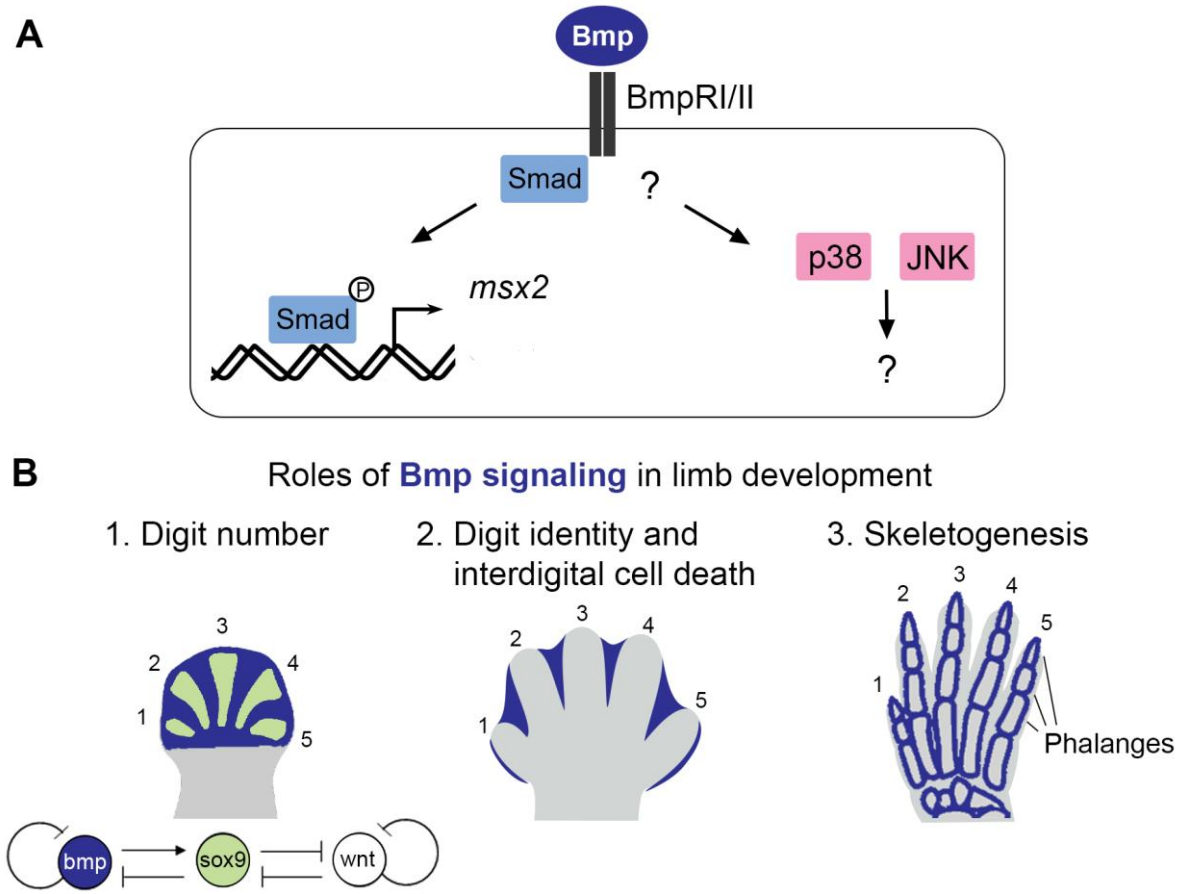

Figure 3. Bmp signaling has multiple roles during limb development.

(**A**) Illustration of the Bmp pathway. When Bmp proteins bind to their receptors, the Smad transcription factors are phosphorylated and translocate to the nucleus, where they activate expression of target genes such as *msx2*. Non-canonical Bmp signaling has also been reported in the limbs, where the Bmp receptors activate the stress-activated MAP kinases p38 and JNK. The role of these MAP kinases in the limbs is unclear. Based on Gunnel et al., 2010 and Pignatti et al., 2014.

(**B**) Bmp signaling has multiple roles during limb development: (1) establishment of the total number of fingers, as a self-patterning mechanism in combination with Wnt signaling and *sox9*; (2) establishment of the digit identity (i.e., the total number of phalanges of each finger) and induction of interdigital cell death; and (3) skeletogenesis. Areas of expression of *bmp* transcripts in the mesenchyme are represented in blue. For further discussion, please see the text. Based on Huang et al., 2016, Raspopovic et al., 2011 and Zuzarte-Luis and Hurle, 2005.

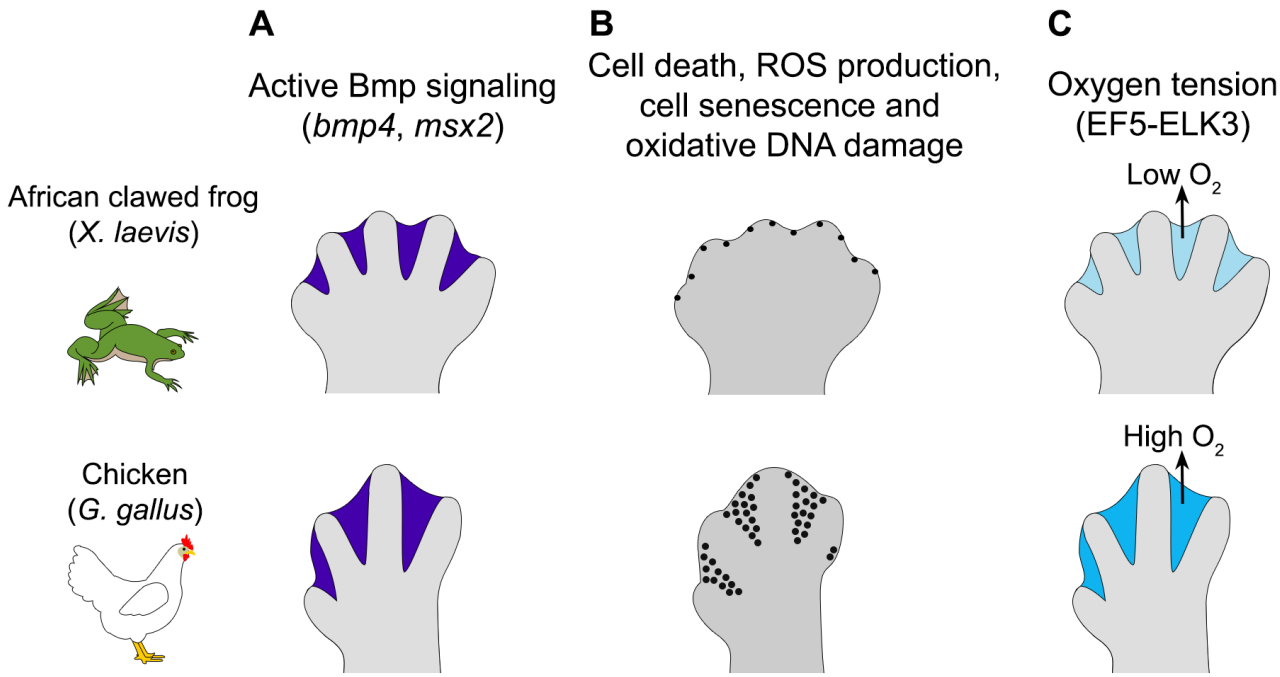

Figure 4. Morphogenesis of chicken and *X. laevis* limbs and the role of oxygen.

(**A**) Bmp signaling is active in the interdigital regions of both *X. laevis* and chicken. Expression of *bmp4* and its target gene *msx2* are found in equivalent stages of the two investigated species.

(**B**) Production of reactive oxygen species (ROS) may lead to oxidation of macromolecules, as indicated by the oxidative DNA damage marker 8-oxoguanine. Oxidative stress may lead to cell senescence and cell death. These features were found throughout the interdigital of chicken limbs, while were restricted to the limb margins of *X. laevis*.

(**C**) EF5 is a chemical that only binds to proteins under hypoxia, and can be detected by the antibody ELK3. Thus, the EF5-ELK3 staining measures the oxygen tension in the tissue. While chicken had high oxygen levels in the interdigital region with no EF5 binding, the interdigital region of *X. laevis* were hypoxic.

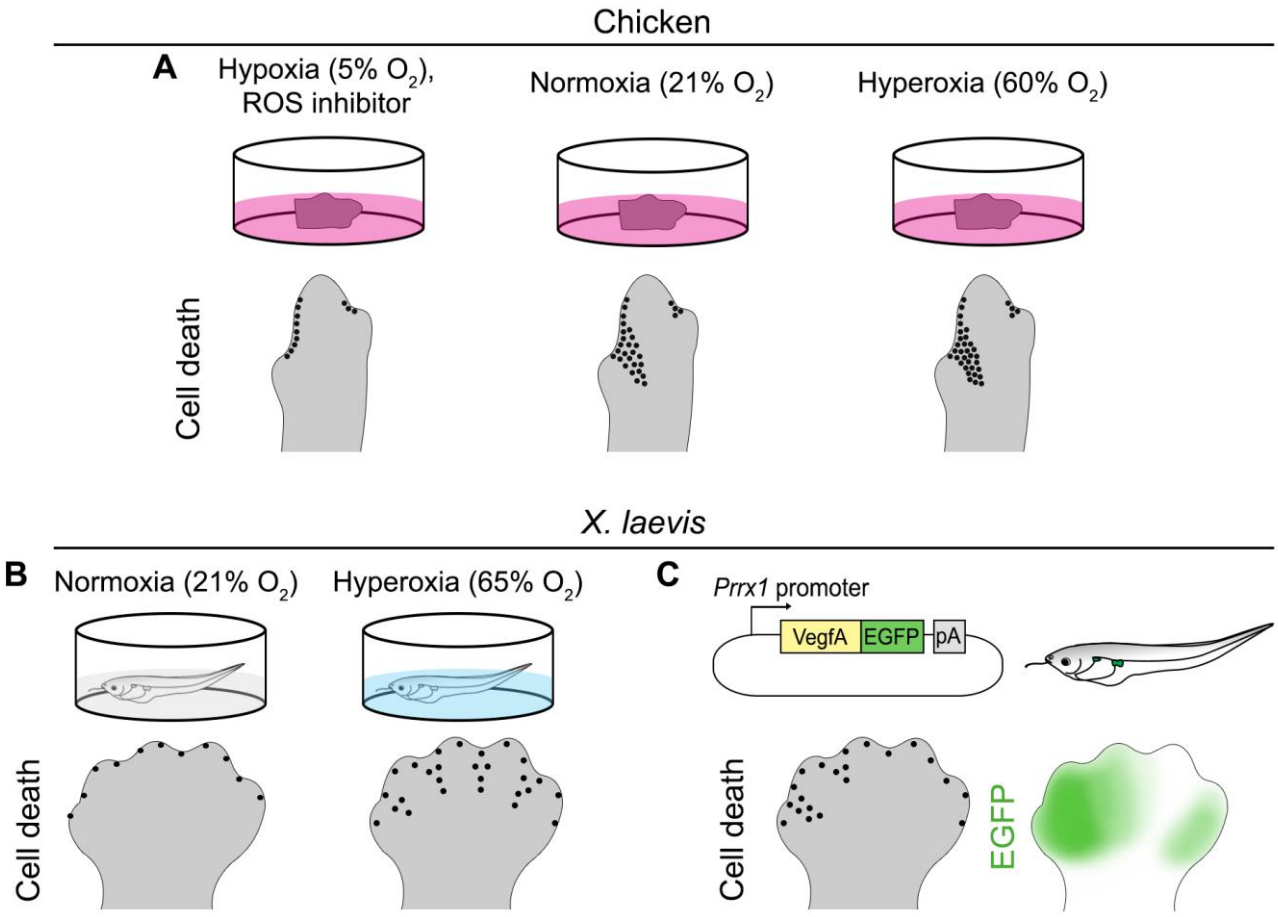

Figure 5. Modulation oxygen levels regulates cell death in the limbs of both chicken and *X. laevis*.

(**A**) Chicken wings were isolated and incubated in culture medium for 6 hours under different oxygen levels. In comparison with control wings incubated under 21% atmospheric oxygen (normoxia), wings incubated with both the ROS inhibitor N-acetyl-cysteine or under low oxygen levels (hypoxia, 5%) had a reduction in interdigital cell death. while Limbs incubated under high oxygen levels (hyperoxia, 65%) had more dying cells in the interdigital region.

(**B**) Whole *X. laevis* tadpoles were incubated under control (normoxia, 21%) or high (hyperoxia, 65%) oxygen levels. Hyperoxia induced cell death specifically in the interdigital regions of the frog's hindlimbs in late stage 54 and stage 55, while the tadpoles under normoxia had cell death only in the limb margins. Increased ROS production was also found under hyperoxia.

(**C**) *Prrx1-VegfA-EGFP* transgenic *X. laevis* tadpoles express the angiogenic factor VegfA fused to the reported EGFP under the control of the limb-specific Prrx1 promoter. A greater blood vessel density is found in these transgenic frogs' limbs. At late stage 54, the expression of the transgene was stronger in the anterior region. The increased number of blood vessels – the sources of oxygen in the tissue – induced interdigital cell death in the anterior region of the hindlimbs.

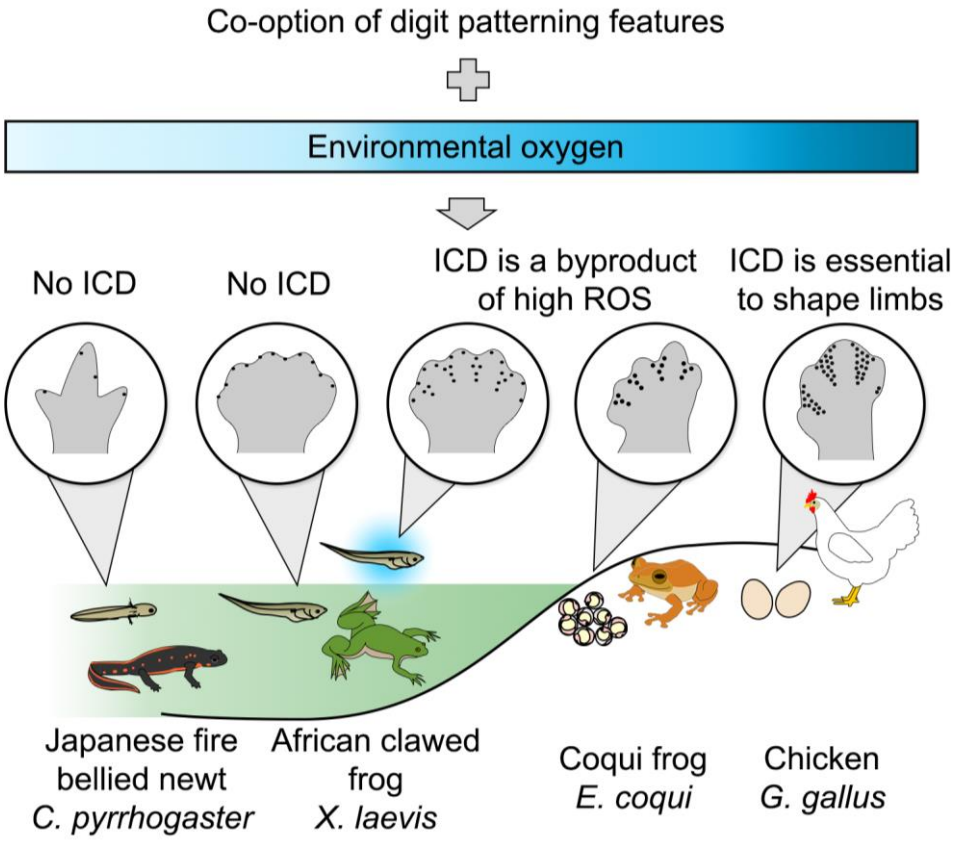

Figure 6. Model of the appearance of interdigital cell death in tetrapod evolution.

The two amphibians investigated here which have aquatic tadpoles – the Japanese fire bellied newt (*Cynops pyrrhogaster*) and the African clawed frog (*Xenopus laevis*) – had no interdigital cell death (ICD). In contrast, ICD was found in limbs of the coqui frogs (*Eleutherodactylus coqui*), which have terrestrial direct-developing embryos. The pattern found in the coqui frog was similar to what was found in a previously investigated direct-developing salamander (*Desmognathus aeneus*, Franssen et al., 2005).

We propose that features important for digit patterning – Bmp signaling and blood vessel remodeling, as illustrated in Figure 7 – made the interdigital regions permissive for the induction of cell death. When environmental oxygen levels are high, ROS are produced by interdigital cells, leading to cell death. It is not clear if the dying cells found in amphibians are integrated with other limb development mechanisms or are only a byproduct of high ROS. During evolution, this novel mechanism became essential to shape amniote limbs.

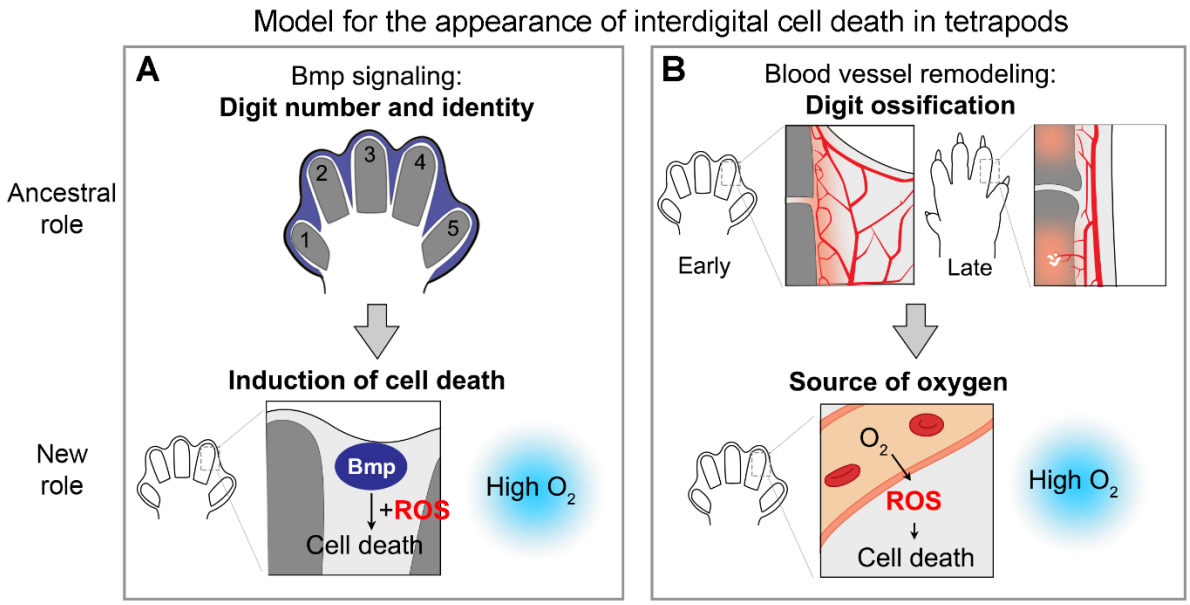

Figure 7. Molecular mechanism for the evolution of interdigital cell death in tetrapods.

(**A**) Interdigital Bmp signaling (blue) is essential for establishing digit number and identity in tetrapods (Figure 3). The same interdigital Bmps also make this region permissive for induction of cell death when sufficient ROS are available.

(**B**) Early finger condensations induce the formation of a rich blood vessel network surrounding digit cartilages. These vessels allow allows a timely vascular invasion of the ossification center and the differentiation into bone. In the autopod, the early remodeling process also increases interdigital blood vessel density, providing an abundant oxygen source linked to ROS production and ICD. Thus, Bmp signaling and blood vessel gained a new role during the evolution.